RSC Advances

ROYAL SOCIETY OF CHEMISTRY

www.rsc.org/advances

Exploration of unconventional π–hole and C–H···H–C types of supramolecular interactions in a trinuclear Cd(II) and a heteronuclear Cd(II)-Ni(II) complex and experimental evidence for preferential site selection of the ligand by 3d and 4d metal ions.

Saikat Banerjee,[a] Antonio Bauzá,[b] Antonio Frontera,*[b] and Amrita Saha*[a]

Abstract

In this present work we report synthesis and structural characterisations of a trinuclear cadmium (II) (**1**) and a di(phenoxido)-bridged dinuclear cadmium(II)–nickel(II) (**2**) complexes derived from a bicompartmental (N2O4) Schiff base ligand, **H_2L**. It has been observed that, in bicompartmental ligands the relatively small inner core is suitable for 3d metal ions and outer core can be occupied by different metal centers like 3d, 1s, 2s, 4d and 4f. We have experimentally established the above fact. In homotrinuclear complex **1** both inner (N2O2) and outer (O4) core has been occupied by cadmium (II) ions. Complex **1** upon reaction with $NiCl_2.6H_2O$ produces heterodinuclar complex **2**. Structural studies reveal that, in complex **1** terminal Cd units acquire trigonal prismatic geometry whereas the central Cd unit is eight coordinated. In case of complex **2** both nickel(II) and cadmium(II) ions are hexa-coordinated in a distorted octahedral environment. Both the complexes are studied using different spectroscopic techniques. Complexes **1** and **2** exhibit important and relatively unexplored group of supramolecular interactions like π–hole, C–H···π and C–H···H–C along with other hydrogen bonding interactions. Theoretical DFT calculations are devoted to analyze these non covalent

interactions. Several computational tools like MEP surface analysis and NCI analysis are utilized to explain and illustrate such interactions.

Introduction

Schiff-base complexes play an important role in the development of modern coordination chemistry and have various applications in the field of magnetism, catalysis, medicinal chemistry, gas storage, electron transport processes and sensing.[1-9] Among the Schiff base ligands acyclic compartmental ligands which contains two different sites are vastly used to prepare homo and heteronuclear complexes. Such types of Schiff base ligands are achieved from the condensation between diamines and salicylaldehyde with an appended alkoxy group at ortho position to the phenoxido oxygen (salphen) (Scheme 1). The ligands have two different tetradentate coordination core, inner core consists of two imine-N and two phenoxo-O atoms and outer core involves two phenoxo-O and two alkoxy-O units. In case of homonuclear complexes large number of di, tri, tetra and polynuclear complexes having 3d and 4d metals[10-12] are known whereas heteronuclear complexes involves different 3d-1s, 3d-2s,[13-19] 3d-3d,[20-36] 3d-4d,[37-38] and 3d-4f metal centers.[39-48]

It has been observed that during formation of homo or heteronuclear complexes bicompartmental ligands first form an intermediate known as “metallo-ligand reactant”. This metallo-ligand system further react with different metals ions with 1s, 2s, 3d, 4d and 4f electronic configuations, ammonium ion, dicarboxylic acid and deprotonated diamine. The mostly used transition metal centre among the divalent first row transition element to prepare “metallo-ligand reactant” is Cu(II). In this case the Cu(II) center is coordinated with two imine-N and two phenoxo-O atoms. Ni(II),[22,26,32] Mn(II)[24] and Zn(II)[39-42] are also used for the same purpose. In this context Salphen complexes containing zinc(II) need special mention. They have

been widely used in the field of supramolecular chemistry,[49] catalysis[50] and transmetalation.[51] Presence of available coordination site and presence of intermolecular Zn···O interactions between the zinc(II) center of a salphen unit and phenolic oxygen of another are the two most dominating facts to exhibit such types of behavior. It has been also observed that zinc salphen moiety incorporated into a crown ether framework exhibit excellent binding affinity toward cationic guest species.[52]

The structural diversity of such complexes are achieved by interesting non covalent interactions like hydrogen bonding, cation–π, anion–π, CH–π[53] and other less recognized forces, such as, σ/π-hole,[54] and C–H···H–C interactions[54] etc. It is now well established that supramolecular interactions deal with weak and reversible non covalent interactions which are the basis of highly specific recognition, transport, and regulation mechanisms. It is vastly used to understand the progress in many biological functions and drug design. Amongst supramolecular interactions σ/π-holes interactions are very important but comparatively unexplored. In 1973 Birgi and Dunitz in a series of work explain the pathway along which a nucleophile attacks the π -hole of a C=O group.[55] It has been observed that in a given group of the periodic table, σ/π-hole interactions become more positive on going from the lower atomic number to the higher atomic number. A positive π-hole interaction is highly directional in nature and observed between a region with positive electrostatic potential of unpopulated π* orbitals and electron dense region. Recently, π -hole interactions has been observed in acyl carbons,[56] SO_2 and SO_3 moieties, [57] RNO_2 molecules,[58] XCN, XZO_2 (X=halogen, Z = pnictogen), etc.[59] It is important to mention that the nitro group plays a crucial role to modify the electronic nature of aromatic rings or aliphatic chains. Therefore, it will participate in π-hole interactions and thus plays an important

role in crystal engineering. Halogen bonding also needs special mention as it is important in the field of biological systems and in the design of new materials.

In this work bicompartmental ligand, **H_2L**(N,N'-bis(3- methoxysalicylidene)propylene-1,3-diamine)upon reaction with $Cd(NO_3)_2.4H_2O$ produced a trinuclear complex $[Cd_3(L)_2(NO_3)_2]$(**1**). This trinuclear complex upon reaction with $NiCl_2.6H_2O$ generate a heterodinuclar Ni(II)-Cd(II) complex i.e. $[\{Ni^{II}L(CH_3OH)_2\}CdCl_2].H_2O$(**2**). In complex **1** Cd(II) ions occupy both the coordination positions of the ligand, in complex **2** the inner Cd(II) centreis easily replaced by the Ni(II) ion. Different spectroscopic studies are used to characterize both the complexes. In contrast to the propensity of Cu(II) complexes to react with a second metal salt, only few products have been obtained from a mononuclear Ni(II) compounds.[11]

Most interesting observation in the supramolecular assembly of complex **1** and **2** is the existence of remarkable π–hole, C–H···π and C–H···H–C interactions along with other hydrogen bonding interactions. In complex **1** π-hole interaction is established between the O atom of the nitrato ligand and the C atom of the C=N bond. Molecular electrostatic potential (MEP) surface analysis and the non covalent interaction (NCI) analysis of compounds **1** and **2** allow an assessment of different nonbonding interactions and the extent to which these weak interactions stabilize the complex. Briefly, the systems derived from the bi compartmental ligand, **H_2L** exhibit in the solid state self-assemblies that are governed by an intricate combination of weak interaction. They are thus interesting in the frontier research area of crystal engineering and supramolecular chemistry. Thus, we have been motivated to explore this area further.

Experimental section

Materials and synthesis

All reagent or analytical grade chemicals and solvents were purchased from commercial sources and used without further purification.

Synthesis of Schiff base ligand **(H_2L = N,N' -bis(3- methoxysalicylidene)propylene-1,3-diamine)**

The tetradentate Schiff base ligand (**H_2L**) was prepared by the standard method.[60] Briefly, a mixture of o-vaniline (8.0 mmol, 1.217 g) and 1,3-diaminopropane (4.0 mmol, 0.296 g) in 50 mL methanol was heated to reflux for 2 h. The resulting light yellow colored Schiff base ligand (**H_2L**) was used for further reaction.

Preparation of $[Cd_3(L)_2(NO_3)_2]$ (1)

A 10 ml methanolic solution of cadmium nitrate (6.0 mmol, 1.848 g) was added to a methanolic solution of H_2L (4.0 mmol) followed by addition of triethylamine (8.0 mmol, ~1.5 mL) and the resultant reaction mixture was heated to reflux for 4 h. The solution was then cooled and filtered. Deep yellow colored crystals resulted from the slow evaporation of methanolic solution of the complex at room temperature. Yield: 0.1880 g (82%). Anal. Calc. for $C_{38}H_{40}Cd_3N_6O_{14}$: C 36.87%; H 3.09%; N 7.82%. Found: C 36.35%; H 3.07%; N 7.29%. IR (cm^{-1}, KBr): υ(C=N) 1625 m; υ(C-N) 1225 s; ν(C-H) 730 s. UV-Vis, λ_{max} (nm), (ε ($dm^3mol^{-1}cm^{-1}$)) in DMF-CH_3CN (1:9, v/v): 268 (10420), 353 (4004).

^{1}H NMR (DMSO-d_6, 300 MHz) δ ppm: 1.81 (bs, 2H), 4.12 (bs, 4H), 6.27-6.9 (m, 4H), 8.17-8.32 (m, 2H)

^{13}C NMR (DMSO-d_6, 75 MHz) δ ppm: 31.98 (-CH_2), 55.6 (-OCH_3), 63.9 (-CH_2), 113.44(-CH), 118.67 (-CH), 128.04 (-CH), 149.73 (-CH), 169.56 (-CH=N).

Preparation of $[\{Ni^{II}L(CH_3OH)_2\}CdCl_2].H_2O$ (2)

A 10 ml methanolic solution of nickel chloride (2.0 mmol, 0.4754 g) was added to a methanolic suspension of complex **1** (1.0 mmol) and the reaction mixture was stirred for 3 h at room temperature. Then the solution was filtered. Deep green colored crystals resulted from the slow evaporation of methanolic solution of the complex at room temperature.

Colour: Deep Green. Yield: 0.0996 g (75%). Anal. Calc. for $C_{21}H_{30}CdCl_2N_2NiO_7$: C 37.96%; H 4.55%; N 4.22%. Found: C 37.20%; H 4.15%; N 4.02%. IR (cm^{-1}, KBr): υ(C=N) 1620 m; υ(C-N) 1217 s; ν(C-H) 737 s. UV-Vis, λ_{max} (nm), (ε ($dm^3mol^{-1}cm^{-1}$)) in DMF-CH_3CN (1:9, v/v): 287 (28878), 370 (2123), 580 (195).

Physical measurements

Elemental analysis for C, H and N was carried out using a Perkin–Elmer 240C elemental analyzer. Infrared spectra (400–4000 cm^{-1}) were recorded from KBr pellets on a Nicolet Magna IR 750 series-II FTIR spectrophotometer. Absorption spectra were measured using a UV-2450 spectrophotometer (Shimadzu) with a 1-cm-path-length quartz cell. Electron spray ionization mass (ESI-MS positive) spectra were recorded on a MICROMASS Q-TOF mass spectrometer. Measurements of ^1H NMR spectra were conducted using a Bruker 300 spectrometer in DMSO-d_6. Emission was examined by LS 55 Perkin–Elmer spectrofluorimeter at room temperature (298 K) in DMSO-Methanol (1:9, v/v) solution under degassed condition.

X-ray crystallography

Single crystal X-ray data of complexes **1** and **2** were collected on a Bruker SMART APEX-II CCD diffractometer using graphite monochromated Mo Kα radiation (λ = 0.71073 Å) at room temperature. Data processing, structure solution, and refinement were performed using Bruker

Apex-II suite program. All available reflections in $2\theta_{max}$ range were harvested and corrected for Lorentz and polarization factors with Bruker SAINT plus.[61] Reflections were then corrected for absorption, inter-frame scaling, and other systematic errors with SADABS.[62] The structures were solved by the direct methods and refined by means of full matrix least-square technique based on F^2 with SHELX-97 software package.[63] All the non hydrogen atoms were refined with anisotropic thermal parameters. C-H hydrogen atoms were inserted at geometrical positions with $U_{iso} = 1/2U_{eq}$ to those they are attached. Crystal data and details of data collection and refinement for **1** and **2** are summarized in Table 1.

Theoretical methods

The calculations of the non covalent interactions were carried out using the TURBOMOLE version 7.0[64] using the BP86-D3/def2-TZVP level of theory. To evaluate the interactions in the solid state, we have used the crystallographic coordinates. This procedure and level of theory have been successfully used to evaluate similar interactions.[65] The interaction energies were computed by calculating the difference between the energies of isolated monomers and their assembly. The interaction energies were corrected for the Basis Set Superposition Error (BSSE) using the counterpoise method.[66]

The NCI plot is a visualization index based on the electron density and its derivatives, and enables identification and visualization of non covalent interactions efficiently. The isosurfaces correspond to both favorable and unfavorable interactions, as differentiated by the sign of the second density Hessian eigenvalue and defined by the isosurface color. NCI analysis allows an assessment of host-guest complementarity and the extent to which weak interactions stabilize a complex. The information provided by NCI plots is essentially qualitative, i.e. which molecular regions interact. The color scheme is a red-yellow-green-blue scale with red for ρ^{+}_{cut} (repulsive)

and blue for ρ^{-}_{cut} (attractive). Yellow and green surfaces correspond to weak repulsive and weak attractive interactions, respectively.[67]

Hirshfeld Surface analysis

Hirshfeld surface analysis have been done using Crystal Explorer version 3.1.[68] The normalized contact distance (d_{norm}) based on d_i and d_e has been determined by the given equation where r^{vdW} is the van der Waals (vdW) radius of the appropriate atom internal or external to the surface.

$$d_{norm}=\frac{(d_i-r_i^{vdW})}{r_i^{vdW}}+\frac{(d_e-r_e^{vdW})}{r_e^{vdW}}$$

d_{norm} becomes negative for shorter contacts than vdW separations and becomes positive for contacts greater than vdW separations, and is displayed using a red–white–blue color scheme, where red highlights shorter contacts, white is used for contacts around the vdW separation, and blue is for longer contacts.[69]

Results and Discussion

Syntheses, IR, UV/Vis spectra, photoluminescence properties of the Complexes

The Schiff base used in this work is a well known symmetrical tetradentate ligand (**H_2L**).[60] One of the important aspects of this type of ligand (salphen) is that upon metalation the phenol oxygen atoms of the ligand become negatively charged phenoxo groups, which have higher coordination ability to another metal ion. Complex **1** was prepared by the reaction of $Cd(NO_3)_2.4H_2O$ with H_2L in 3:2 molar ratio in methanol in presence of few drops of trimethyl amine. Complex **2** was prepared by mixing complex **1** with $NiCl_2{\cdot}4H_2O$ in methanol in a 1:1 molar ratio as shown in Scheme 1. Besides elemental analysis, all of the complexes were initially characterized by IR spectroscopy. A strong and sharp band appeared at 1634 and 1619 cm^{-1},

respectively for complex **1** and **2**, due to azomethine υ(C=N). In complex **1**, stretching frequencies at 1385 and 1290 cm^{-1} were tentatively assigned to $\nu(NO_3^-)$. In complex **2**, a broad band appeared at 3443 cm^{-1}, which may be assigned to the O–H stretching of the MeOH or of the crystallized water molecule. The electronic spectra of complexes **1** and **2** are recorded in DMF-CH_3CN (1:9 v/v) mixture of solvent. Both the complexes exhibit two sharp absorption bands around 270 nm and 350 nm. These absorption bands can be assigned to n → π* or π → π* transitions of the Schiff-base ligands. Besides these bands, a broad absorption band is observed in the visible region for complex **2** at 580 nm which can be assigned to the spin-allowed d-d transition $^3T_{1g}(F) \leftarrow {}^3A_{2g}$.[70] ^1H NMR spectrum of complex **1** was performed using d_6-DMSO as solvent. For complex **1** aromatic protons appeared within 6.27-6.90 ppm, where as aliphatic protons appeared around 4.32 ppm and 1.80 ppm respectively. Azomethine CH=N proton appeared at 8.3 ppm. In ^{13}C NMR spectrum of complex **1**, the aromatic carbon atoms appeared within 113-118 ppm. Whereas, the imine carbon atom (-CH=N) appeared at 169.53 ppm. Aliphatic carbon atoms and carbon atom of the methoxy group appeared around 31, 63 and 55 ppm respectively. (Figure S3-S6) Fluoresence spectrum of the free ligand complex **1** and **2** were performed in DMF-CH_3CN (1:9 v/v) mixture of solvent. Free ligand $\mathbf{H_2L}$ upon excitation gives a broad fluorescent emission band at 458 nm. Complex **1** upon excitation at 353 nm gives an intense emission peak was observed at 492 nm.(Figure 3) This type of luminescence may be attributed to the intraligand (π → π*) transition and the red shift in complex **1** may presumably be due to the metal coordination.[71-76] For complex **2**, upon excitation at 287 nm and 370 nm respectively, no significant fluorescent emission band was observed mainly due to presence of Ni(II) ion in the moiety.

Description of the crystal structures of $[Cd_3(L)_2(NO_3)_2]$ (1)

Compound **1** crystallized from slow diffusion of methanol solvent and it has monoclinic space group P21/c. The crystal structure of $[Cd_3(L)_2(NO_3)_2]$ (**1**) is presented in Figure 1. Selected bond lengths and angles for complex **1** are given in table 2. The core structure of **1** contains a Cd3 unit. The two terminal Cd atoms Cd1 and Cd2 are located in the inner N2O2 cavities of the two Schiff base ligands and are each bonded to a bidentate nitrate anion, resulting in a trigonal prismatic geometry. Both Cd1 and Cd2 atoms lie slightly above the N2O2 plane by 0.792 A°. The central metal atom Cd3 is eight coordinated and is encapsulated in the O8 cavity formed by four phenolic oxygen atoms (O,O) and four methoxy oxygen atoms (O,O). Thus the bridging phenoxo oxygen atoms of the deprotonated Schiff base ligand L^{2-} connect each terminal Cd atom to the central Cd atom forming bis(μ-phenoxo) bridged Cd(II) - Cd(II) motifs. The three Cd(II) ions are nearly linear with a Cd(1)-Cd(3)-Cd(2) angle of 172.34° and Cd-Cd distances are similar 3.556Å and 3.546 Å for Cd1-Cd3 and Cd3-Cd2 respectively. The Cd-N, Cd-O (phonolic), Cd-O (methoxy) bond distances are 2.249 Å, 2.242 Å and 2.63 Å respectively and these values are comparable with those found in other Schiff base complexes of Cd.[11] The Cd-O bond distances varies in the extensive range which indicate different types of interaction between the Cd(II) ion and the O atoms within the molecule. Presence of three carbon backbone makes the ligand flexible and the two N2O2 planes of the Schiff base are crossed with dihedral angles of 66.77° respectively.

In complex **1** self assembly by week π-hole interactions is observed. Cadmium coordinated nitrate ions interact with imine C-H moieties through delocalized π- electron cloud. As a result one trinuclear unit is interlinked with two neighboring trinuclear units to generate a two dimensional sheet. Presence of π…π interactions between phenyl rings of same molecule

(intramolecular) and two adjacent molecules (intermolecular) further stabilizes the structure. The distance between the centers of two rings is 3.952 Å.

Description of the crystal structures of [{$Ni^{II}L(CH_3OH)_2$}$CdCl_2$].H_2O (2)

Compound **2** crystallized from slow diffusion of methanol solvent and it has monoclinic space group $P2_1/n$. A perceptive view and atom numbering scheme of the asymmetric unit of [{$Ni^{II}L(CH_3OH)_2$}$CdCl_2$].H_2O (**2**) is presented in figure 2. Selected bond lengths and angles of complex **2** are given in table 3. One molecule of complex **1** upon reaction with $NiCl_2.6H_2O$ generates complex **2**. Monomeric unit of Complex **2** consists of one [NiL] unit, one cadmium ion, two chloride anions and two methanol molecule. In the structure a crystallographic two fold axis passes through the cadmium atom. Crystal structure clearly reveals that the Ni(II) ion has replaced the Cd(II) from the inner core of the Schiff base ligand of complex **1**. Ni(II) ion is present in a hexa coordinated octahedral geometry where the basal plane is formed by the two imine N atoms N(1) and N(2), and two phenoxido O atoms O(1) and O(3), of the schiff base. Two methanol molecules coordinated axially to the metal centre (O5, O6) through the oxygen center to complete the coordination. The Cd(II) molecule is present as a terminal unit where it is coordinated with two phenolic oxygen atoms (O1,O3), two methoxy oxygen atoms (O2,O4) of the Schiff base ligand and two chloride ions resulting a highly distorted octahedral geometry. The bridging phenoxo oxygen atoms of the deprotonated Schiff base ligand L^{2-} connect terminal Cd atom to the Ni(II) atom forming bis(μ-phenoxo) bridged Cd(II) - Ni(II) motif with metal metal separation of 3.390Å. Terminal Cd-phenoxo bond distances (2.2595Å) are significantly shorter than the Cd-methoxy bond distances (2.5265Å). Whereas Cd-Cl bond distances (2.4667Å) are shorter than the corresponding Cd-methoxy bond

distances but longer than the Cd-phenoxo bond distances. The small value of the average deviation of the four oxygen atoms from the least square O4 plane clearly suggests that the four oxygen atoms of O-phenoxo and O-methoxy unit exists in almost planer form. The displacement of Cd(1) from the least square O4 plane is 0.082 Å which suggests that the metal is perfectly placed inside the O4 compartment. The range of bond angle around the Cd center are 65.39(8)–159.99(8)°. The Ni-imine (2.026(3) Å and 2.033(3) Å) and Ni-phenoxo (2.003(2)Å and 1.993(2)Å) bond distances which lie in the usual range[32] are shorter than the Ni-O (methanol) bond distances (2.142(3)Å and 2.158(3)Å respectively). The small value of the average deviation of the four oxygen atoms from the least square N2O2 plane clearly suggests that the four oxygen atoms of O-phenoxo and O-methoxy unit exists in almost planer form. The displacement of Ni(1) from the least square N2O2 plane is 0.013 Å which suggests that the metal is perfectly placed inside the N2O2 compartment. This result clearly suggests that small size of Ni(II) center has more preference towards the inner core compared to the relatively large Cd(II) ion.

The orientation of ligands around the metal center is such that is no π-π stacking interaction is observed. But the molecule displays various interesting hydrogen bonding interactions. The molecule contains water molecule as solvent of crystallization. It exhibits both intramolecular and intermolecular hydrogen bonding with Ni-coordinated methanolic O-H and Cd-coordinated chlorine atoms and thus forming 2D sheet in bc plane.

Computational Study

The theoretical study is devoted to analyze the non covalent interactions that govern the crystal packing of compounds **1** and **2** focusing our attention to the remarkable π–hole, C–H···π and C–H···H–C interactions. In **1**, the absence of good H-bond donors facilitates the formation of a π-hole bonding interaction involving the C atom of the C=N bond and the nitrate. This type of

bonding has attracted attention to the scientific community in the last years[77] and has been analyzed in the present study along with other interactions. In **2**, the conventional H-bonding interactions are important due to the presence of the coordinated MeOH that is a very good H-bond donor.

In Figure 4 we show the representation of an infinite chain found in the solid state of compound **1** where interesting and unconventional interactions are established. Apart from long range van der Waals interactions between the organic ligands, two additional interactions are present. One of both is a π-hole interaction between the O atom of the nitrato ligand and the C atom of the C=N bond. The O···C distance is slightly shorter (3.20 Å) than the sum of van der Waals radii (i.e., 3.22 Å). The importance of π-hole interactions in crystal engineering and other fields have been recently reviewed.[54] We have computed the MEP surface of a theoretical model that consists of the Schiff-base ligand used in this work coordinated to a Cd(II) metal center. The MEP surface of this simple model shows a positive electrostatic potential over the C atom of the C=N bond, therefore it is well suited for interacting with electron rich molecules, thus explaining the formation of the π-hole interaction in **1**. The second interaction that we focus our attention is established between two aromatic H atoms and the nitrato ligand (Figure 4A). This interaction can be viewed as C–H···O hydrogen bonding interactions; however the directionality (perpendicular approach) does not correspond to a hydrogen bond. Certainly, it resembles a T-shape stacking interaction, where the π-system of the nitrate anion is involved. To evaluate the unconventional interactions observed in **1**, we have used two theoretical models that are shown in Figure 4C, D. In the first theoretical model (Figure 4C), both π-hole and C–H···NO_3 interactions are evaluated along with other long range van der Waals interactions. The computed interaction energy is ΔE_3 = –27.7 kcal/mol confirming the importance of this intricate

combination of interactions. In the second model the nitrato ligand has been substituted by nitrito (see small arrow in Figure 4D) and, consequently, the π–hole interaction is not formed. The interaction energy is reduced to ΔE_4 = –24.3 kcal/mol. The contribution the π–hole interaction can be evaluated by difference, which is $\Delta E_3 – \Delta E_4$ = –3.4 kcal/mol, confirming its importance in the crystal packing of compound **1**. In order to characterize the interactions in **1**, we have also computed the NCI plot that is shown in Figure 4E. A small green isosurface can be observed between one oxygen atom of the nitrito ligand and the C atom of the C=N bond, thus confirming the existence of the π-hole interaction. More extended surfaces can be observed between the aromatic rings and other aliphatic groups that characterize the long range van der Waals interactions. Moreover, another isosurface is observed between the nitrato ligand and both C–H aromatic groups (Figure 4E). This surface is extended all over the nitrato ligand instead of the formation of two small isosurfaces between the H and O atoms. This indicates that the interaction cannot be defined as H-bonding and, instead, it is better described as a C–H···π interaction involving the whole π-system of the electron rich nitrato ligand.

In Figure 5 we show the representation of self-assembled dimer found in the solid state of compound **2** that is governed by two symmetrically related O–H···Cl interactions. Moreover the methyl groups of the MeOH ligands form C–H···π interactions (at 2.61 Å of the closest C atom of the ring). C–H···H–C interactions are likely present involving the H-atoms of the methyl groups since they are close to each other. The C–H···H–C interaction has been recently studied in depth by Alvarez and coworkers.[54] Although dihydrogen contacts in alkanes are among the weakest intermolecular interactions (~−0.4 kcal/mol for methane dimer), these interactions are cumulative and resulting in larger dimerization energies in some cases (e.g. long open chains).

For instance the complexation energy computed for the dimer of *n*-hexane is −4.5 kcal/mol.[77] In addition, the association energies for dimers of some polyhedranes (tetrahedrane, adamantane, octahedrane, cubane and dodecahedrane) are also strong, reaching −3.0 kcal/mol for dodecahedrane.[77] We have computed the molecular electrostatic potential MEP surface of compound **2** in order to rationalize the formation of the electrostatically driven interactions (see Figure 5B). It can be observed that the most positive region corresponds to the hydroxyl group of the MeOH due to the enhancement of the acidity of the H atom upon coordination to Ni(II). Moreover, the most negative region correspond to the chlorido ligands thus the formation of the O–H···Cl H-bond is electrostatically very favored.

To evaluate the intricate combination of interactions observed in the self-assembled dimer of **2**, we have used several theoretical models (using the crystallographic coordinates) that are shown in Figure 5C, D. We have used DFT calculations at the BP86-D3/def2-TZVP level of theory since it is a good compromise between the accuracy of the method and the size of the system. The interaction energy of the self-assembled dimer (ΔE_1 = –35.6 kcal/mol, Figure 5B) is very large basically due to the contribution of both H-bonding interactions. In an effort to estimate the contribution of the weak C–H···π and C–H···H–C interactions, we have computed an additional model where the methanol molecules have been replaced by water ligands (see small arrows Figure 5D). As a result the interaction is reduced to ΔE_2 = –29.8 kcal/mol that is the contribution of the H-bonding interactions, confirming their strong nature as anticipated by the MEP analysis. The contribution of the weaker C–H···π and C–H···H–C interactions can be estimated by difference, which is –5.8 kcal/mol. In order to characterize the interactions shown in Figure 5, we have computed the non covalent interaction (NCI) plot of this compound. The NCI plot is a visualization index that enables identification and visualization of non covalent interactions

efficiently. The NCI analysis allows an assessment of host–guest complementarity and the extent to which weak interactions stabilize a complex. The information provided is essentially qualitative, that is, which molecular regions interact. The representation of the NCI plot computed for compound **2** is shown in Figure 5E. An extended region can be observed between the aromatic rings and the methyl groups of the methanol ligands, thus characterizing the C–H···π interaction (the green surface corresponds to weak interaction). Small isosurfaces are also present between the chlorido and the hydroxyl groups that confirm the existence of both hydrogen bonding interactions. Finally, a green isosurface is also observed between the methyl groups that confirm the existence of the C–H···H–C interactions.

Hirshfeld Surface analysis

Supramolecular interactions are further investigated using Hirshfeld Surface analysis. Complexes **1** and **2** are mapped over d_{norm} (range of -0.1 to 1.5Å), shape index (range of -1.0 – 1.0Å) and curvedness (range of -4.0 – 0.4) respectively and presented in figure 6 and figure S7 respectively. During mapping surfaces are kept transparent for visualization of different supramolecular interactions. For Complex **1**, H-bonding interactions between the O atom of nitrate ion and H atoms of aromatic ring of *o*-vaniline has been predominantly found as bright red area in the Hirshfeld surfaces. Other longer and weaker interactions appeared as light colour in the surfaces. Fingerprint plots consist of all type of intermolecular interactions. So, fingerprint plots need to be decomposed to have idea of individual contacts. In the decomposed fingerprint plot, complementary regions are obtained where one molecule acts as a donor (de > di) (bottom left of fingerprint plot) and the other as an acceptor (de < di) (bottom right of fingerprint plot). For complex **1**, O...H/H...O, N...H/H...N and H…H contacts comprise 29.7%, 2.8% and 46.1% of the total Hirshfeld surface where O···H interactions comprise around 14.3% of the total Hirshfeld

surface and the H···O interactions comprise around 15.4% of the total Hirshfeld surface. In the decomposed fingerprint plot of complex **1**, O···H interactions are represented by a spike (d_i = 0.92 Å, d_e = 1.22 Å) in the bottom left (donor) area where as H···O interactions are represented by a spike (d_i = 1.21 Å, d_e = 0.91 Å) in the bottom right (acceptor) region (Figure S8).For complex **2**, O...H/H...O, Cl...H/H...Cl and H…H contacts comprise 5.4%, 15.9% and 57.8% of the total Hirshfeld surface where Cl···H interactions comprise around 6.3% of the total Hirshfeld surface and the H···Cl interactions comprise around 9.6% of the total Hirshfeld surface. In the decomposed fingerprint plot of complex **2**, Cl···H interactions are represented by a spike (d_i = 0.85 Å, d_e = 1.45 Å) in the bottom left (donor) area where as H···Cl interactions are represented by a spike (d_i = 1.44 Å, d_e = 0.86 Å) in the bottom right (acceptor) region (Figure S8).

Life Time Measurements

Lifetime data of the complex **1** was studied at 298 K in acetonitrile solution upon excited at 368 nm. The average fluorescence decay life time has been measured for the complex **1** using the given formula ($\tau_f = a_1\tau_1 + a_2\tau_2$, where a_1 and a_2 are relative amplitude of decay process). The average fluorescence lifetime of complex is 0.3244 nSec. (Figure 7, Table S1)

Concluding remarks

We have synthesized and structurally characterized one trinuclear cadmium (II) (**1**) and one di(phenoxido)-bridged dinuclearcadmium(II)–nickel(II) (**2**) complexes derived from a bicompartmental (N2O4) Schiff base ligand. Crystal structure of complex **2** has proved preferential selection of inner core of the N2O4 donor Schiff base ligand by 3d metal ion in comparison with a 4d metal ion. The supramolecular assemblies observed in the solid state

architectures of both complexes features have been further investigated theoretically using DFT calculations. Supramolecular structure of complex **1** exhibits remarkable π–hole and C–H···π interactions. Moreover, complex **2** exhibits weak C–H···H–C interactions between H-atoms of closely spaced methyl groups along with other non-covalent interactions. The theoretical study,by means of the NCI plot, has confirmed the existence of these interactions which have been rationalized using MEP surfaces. More importantly, we have calculated the energetic contribution of each interaction, which can be helpful to develop scoring functions. Hirshfeld surface mapping and fingerprint plotting have been done to visualize the close contacts qualitatively.

Acknowledgment

A. S. gratefully acknowledges the financial support of this work by the DST, India (Sanction No. SERB/F/1855/2015-16 date 04/07/2015) and Innovative Research Activity under XII Plan General Development Assistance, UGC. The authors also acknowledge the use of the DST-funded National Single Crystal X-ray Diffraction Facility at the Department of Chemistry, Jadavpur University, Kolkata-700032, India for X-ray crystallographic studies. A. F. gratefully acknowledges the financial support of this work by the DGICYT of Spain (projects CTQ2014-57393-C2-1-P and CONSOLIDER INGENIO 2010 CSD2010-00065, FEDER funds). A. F. thanks the CTI (UIB) for free allocation of computer time.

Appendix A. Supplementary data

CCDC 1062044-1062045 contain the supplementary crystallographic data for complexes **2** and **1** respectively. These data can be obtained free of charge via http://www.ccdc.cam.ac.uk/conts/retrieving.html, or from the Cambridge Crystallographic Data Centre, 12 Union Road, Cambridge CB2 1EZ, UK; fax: (+44) 1223-336-033; or email:deposit@ccdc.cam.ac.uk.

Notes & References

[a]*Department of Chemistry, Jadavpur University, Kolkata- 700032, India.*

E-mail: asaha@chemistry.jdvu.ac.in; amritasahachemju@gmail.com;Tel. +91-33-2457294

[b]*Departament de Química, Universitat de les Illes Balears, Crta. De Valldemossa km 7.5, 07122 Palma (Baleares), Spain.*

E-mail: toni.frontera@uib.es.

[1] E. Tsuchida, K. Oyaizu, *Coord. Chem. Rev*., 2003, **237**, 213.

[2] L. Canali and D. C. Sherrington, *Chem. Soc. Rev*., 1999, **28**, 85.

[3] J. Tisato, F. Refosco and F. Bandoli, *Coord. Chem. Rev*., 1994, **135**, 325.

[4] C. Adhikary, S. Koner, *Coord. Chem. Rev.*, 2010, **254**, 2933.

[5] K.C. Gupta, A.K. Sutar, *Coord. Chem. Rev*., 2008, **252**, 1420.

[6] K.L. Gurunatha, T.K. Maji, *Inorg. Chem*., 2009, **48**, 10886.

[7] T.K. Maji, G. Mostafa, R. Matsuda, S. Kitagawa, *J. Am. Chem. Soc*., 2005, **127**, 17152.

[8] E.C. Niederhoffer, J.H. Timmons, A.E. Martell, *Chem. Rev*., 1984, **84**, 137.

[9] M.D. Allendorf, C.A. Bauer, R.K. Bhakta, R.J.T. Houk, *Chem. Soc. Rev*., 2009, **38**, 1330.

[10] S. Thakurta, C. Rizzoli, R.J. Butcher, C.J. Gómez-García, E. Garribba, S.Mitra, *Inorganica Chimica Acta*, 2010, **363**, 1395.

[11] K. Agapiou, M.L. Mejía, X. Yang, B.J. Holliday, *Dalton Trans.,* 2009, 4154.

[12] S. Thakurta, J. Chakraborty, G. Rosair, J. Tercero, M.S. El Fallah, E. Garribba, S. Mitra, *Inorg. Chem*., 2008, **47**, 6227.

[13] F. Franceschi, E. Solari, R. Scopelliti, C. Floriani, *Angew. Chem*. *Int. Ed*., 2000, **39**, 1685.

[14] T. Fujinami, R. Kinoshita, H. Kawashima, N. Matsumoto, J.H. Harrowfield, Y. Kim, *J. Incl. Phenom*. *Macrocycl. Chem.,* 2011, **71**, 463.

[15] D. Cunningham, P. McArdle, M. Mitchell, N.N. Chonchubhair, M. O'Gara, F. Franceschi, C. Floriani, *Inorg. Chem*., 2000, **39**, 1639.

[16] M. Mousavi, V. Bereau, J.-P. Costes, C. Duhayon, J.-P. Sutter, *CrystEngComm.,* 2011, **13,** 5908.

[17] F.Z.C. Fellah, J.-P. Costes, F. Dahan, C. Duhayon, J.-P. Tuchagues, *Polyhedron*, 2007, **26,** 4209.

[18] S. Sarkar, S. Mohanta, *RSC Adv*., 2011, **1**, 640.

[19] S. Hazra, S. Sasmal, M. Nayak, H.A. Sparkes, J.A.K. Howard, S. Mohanta, *CrystEngComm.,* 2010, **12**, 470.

[20] A.D. Khalaji, H. Stoekli-Evans, *Polyhedron,* 2009, **28,** 3769.

[21] K. Kubono, K. Tani, K. Yokoi, *Acta Crystallogr., Sect. E*, 2012, **68**, m1430.

[22] P. Seth, L. K. Das, M. G. B. Drew, and A. Ghosh, Eur. *J. Inorg. Chem.,* 2012, 2232.

[23] B. Gillon, C. Cavata, P. Schweiss, Y. Journaux, O. Kahn, D. Schneider, *J. Am. Chem. Soc*., 1989, **111**, 7124.

[24] D.-H. Shi, Z.-L. You, C. Xu, Q. Zhang, H.-L. Zhu, *Inorg. Chem. Commun.,* 2007, **10**, 404.

[25] A. Gutierrez, M.F. Perpinan, A.E. Sanchez, M.C. Torralba, M.R. Torres, *Inorg. Chim. Acta,* 2010, **36**, 1837.

[26] S. Oz, J. Titiš, H. Nazir, O. Atakol, R. Boc˘a, I. Svoboda, H. Fuess, *Polyhedron*, 2013, **59**, 1.

[27] R. Ruiz, F. Lloret, M. Julve, J. Faus, M.C. Munoz, X. Solans, *Inorg. Chim. Acta*, 1993, **213**, 261.

[28] S. Oz, R. Kurtaran, C. Arici, U. Ergun, F.N.D. Kaya, K.C. Emregul, O. Atakol, D. Ulku, *J. Therm. Anal. Calorim*., 2010, **99**, 363.

[29] A. Biswas, M. Ghosh, P. Lemoine, S. Sarkar, S. Hazra, S. Mohanta, *Eur. J. Inorg. Chem.,* 2010, 3125.

[30] D.G. Branzea, A. Guerri, O. Fabelo, C. Ruiz-Perez, L.-M. Chamoreau, C. Sangregorio, A. Caneschi, M. Andruh, *Cryst. Growth Des*., 2008, **8**, 941.

[31] M. Nayak, R. Koner, H.-H. Lin, U. Florke, H.-H. Wei, S. Mohanta, *Inorg. Chem*., 2006, **45**, 10764.

[32] P. Chakraborty, S. Mohanta, *Polyhedron*, 2015, **87**, 98.

[33] A. Jana, R. Koner, T. Weyhermueller, P. Lemoine, M. Ghosh, S. Mohanta, *Inorg. Chim. Acta*, 2011, **375**, 263.

[34] L.K. Das, S.-W. Park, S.J. Cho, A. Ghosh, *Dalton Trans.,* 2012, **41**, 11009.

[35] S. Biswas, S. Naiya, C.J. Gómez-García, A. Ghosh, Dalton Trans., 2012, **41**, 462.

[36] A. Chakraborty, B.K. Ghosh, J. Ribas-Arino, J. Ribas, T.K. Maji, *Inorg. Chem*., 2012, **51**, 6440.

[37] J.-P. Sutter, S. Dhers, R. Rajamani, S. Ramasesha, J.-P. Costes, C. Duhayon, L.Vendier, *Inorg. Chem*., 2009, **48**, 5820.

[38] R. Maurice, L. Vendier, J.-P. Costes, *Inorg. Chem*., 2011, **50**, 11075.

[39] H. Wang, D. Zhang, Z.–H. Ni, X.u. Li, L. Tian, J. Jiang, *Inorg. Chem*., 2009, **48**, 5946.

[40] S. Hino, M. Maeda, K. Yamashita, Y. Kataoka, M. Nakano, T. Yamamura, H. Nojiri, M. Kofu, O. Yamamurod, T. Kajiwara, *Dalton Trans*., 2013, **42**, 2683.

[41] M. Maeda, S. Hino, K. Yamashita, Y. Kataoka, M. Nakano, T. Yamamura, Takashi Kajiwara, *Dalton Trans*., 2012, **41**, 13640.

[42] X. Yang, R.A. Jones, V.Lynch, M.M. Oye, Archie L. Holmes, *Dalton Trans.,* 2005, 849.

[43] F. Cimpoesu, F. Dahan, S. Ladeira, M. Ferbinteanu, J.-P. Costes, *Inorg. Chem.,* 2012, **51,** 11279.

[44] J.-P. Costes, T. Yamaguchi, M. Kojima, L. Vendier, *Inorg. Chem*., 2009, **48**, 5555.

[45] J.-P. Costes, B. Donnadieu, R. Gheorghe, G. Novitchi, J.-P. Tuchagues, L. Vendier, *Eur. J. Inorg. Chem*., 2008, 5235.

[46] S. Dhers, S. Sahoo, J.-P. Costes, C. Duhayon, S. Ramasesha, J.-P. Sutter, *CrystEngComm*., 2009, **11**, 2078.

[47] A. Jana, S. Majumder, L. Carrella, M. Nayak, T. Weyhermueller, S. Dutta, D. Schollmeyer, E. Rentschler, R. Koner, S. Mohanta, *Inorg. Chem.,* 2010, **49**, 9012.

[48] R. Koner, G.-H. Lee, Y. Wang, H.-H. Wei, S. Mohanta, *Eur. J. Inorg. Chem*., 2005, 1500.

[49] A.W. Kleij, M. Lutz, A.L. Spek, P.W.N. M. van Leeuwen and J.N.H. Reek, *Chem. Commun.*, 2005, 3661; b) S.J. Wezenberg, E.C. Escudero-Ad´an, J. Benet-Buchholz and A.W. Kleij, *Chem.Eur. J.*, 2009, **15**, 5695; c) M. Kuil, I. M. Puijk, A. W. Kleij, D. M. Tooke, A. L. Spek and J.N.H. Reek, *Chem. Asian J.*, 2009, **4**, 50; d) S. Akine, Y. Morita, F. Utsuno, and T. Nabeshima, *Inorg. Chem.,* 2009, **48**, 10670; e) J.K.-H. Hui and Mark J. MacLachlan, *Dalton*

Trans., 2010, **39**, 7310; f) A.C.W. Leung, J.K.-H. Hui, J. H. Chong and M.J. MacLachlan, *Dalton Trans.*, 2009, 5199; g) P.D. Frischmann, A.J. Gallant, J.H. Chong, and M.J. MacLachlan, *Inorg. Chem*., 2008, **47**, 101.

[50] P.G. Cozzi, *Angew. Chem., Int. Ed.*, 2003, **42**, 2895; F.H. Zelder and J. Rebek Jr., *Chem. Commun.*, 2006, 753.

[51] E.C. Escudero-Ad´an, J. Benet-Buchholz and A.W. Kleij, *Inorg. Chem.*, 2007, **46**, 7265.

[52] a) S.J. Wezenberg, A.W. Kleij, *Angew. Chem., Int. Ed.,* 2008, **47**, 2354; b) A.W. Kleij, *Chem. Eur. J.,* 2008, **14**, 10520; c) H.L.C. Feltham,; S. Brooker, *Coord. Chem. Rev.,* 2009, **253**, 1458; d) A.W. Kleij, *Dalton Trans.,* 2009, 4635; e) S. Akine,; T. Nabeshima, *Dalton Trans.,* 2009, 10395; f) M. Yamamura, H. Miyazaki, M. Iida, S. Akine, and T. Nabeshima , Inorg. Chem., 2011, **50**, 5315.

[53] a) J. Miao, Y. Nie, C. Hub, Z. Zhang, G. Li, M. Xu and G. Sun, *J. Mol. Struct.,* 2012, **97**, 1014; b) C. A. Bessel, R. F. See, D. L. Jameson, M. R. Churchill and K. J. Takeuchi*, J. Chem. Soc., Dalton Trans.,* 1992, 3223; c) K. F. Bowes, I. P. Clark, J. M. Cole, M. Gourlay, A. M. E. Griffin, M. F. Mahon, L. Ooi, A. W. Parker, P. R. Raithby, H. A. Sparkes and M. Towrie, *CrystEngComm,* 2005, **7**, 269; d) J. E. Beves, P. Chwalisz, E. C. Constable, C. E. Housecroft, M. Neuburger, S. Schaffner and J. A. Zampese, *Inorg. Chem. Commun.,* 2008, **11**, 1009; e) S. K. Dey and G. Das, *Cryst. Growth Des.,* 2010, **10**, 754.

[54] a) A. Bauzá, T. J. Mooibroek, A. Frontera, *ChemPhysChem.,* 2015, **16**, 2496; b) J. Echeverría, G. Aullón, D. Danovich, S. Shaik, S. Alvarez, *Nat. Chem.,* 2011, **3**, 323; c) D. Danovich, S. Shaik, F. Neese, J. Echeverría, G. Aullón, S. Alvarez, *J. Chem. Theory Comput.*, 2013, **9**, 1977.

[55] a) H.B. Burgi, *Inorg. Chem.,* 1973, **12**, 2321; b) H.B. Burgi, J.D. Dunitz, E. Shefter, *J. Am. Chem. Soc.,* 1973, **95**, 5065; c) H.B. Burgi, J.D. Dunitz, J.M. Lehn, G. Wipff, *Tetrahedron*, 1974, **30**, 1563.

[56] P. Sjoberg, P. Politzer, *J. Phys. Chem.,* 1990, **94**, 3959.

[57] L.M. Azofra, I. Alkorta, S. Scheiner, *Theor. Chem. Acc*., 2014, **133**, 1586.

[58] a) A. Bauzá, R. Ramis, A. Frontera, *J. Phys. Chem. A*, 2014, **118**, 2827; b) A. Bauzá, T. J. Mooibroek, A. Frontera, *Chem. Commun*., 2015, **51**, 1491.

[59] a) G.S. nchez-Sanz, C. Trujillo, M. Solimannejad, I. Alkorta, J. Elguero, *Phys. Chem. Chem. Phys.,* 2013, **15**, 14310; b) J.E. Del Bene, I. Alkorta, J. Elguero, *J. Phys. Chem. A*, 2013, **117**, 6893.

[60] a) M.G.B. Drew, R.N. Prasad, R.P. Sharma, *Acta Crystallogr. Sect. C*, 1985 **41** 1755; b) K. Iida, I. Oonishi, A. Nakahara, Y. Komoyama, *Bull. Chem. Soc. Jpn.,* 1970, **43,** 2347.

[61] G.M. Sheldrick, SAINT, Version 6.02, SADABS, Version 2.03, Bruker AXS Inc., Madison, Wisconsin, 2002.

[62] G.M. Sheldrick, SADABS: Software for Empirical Absorption Correction, University of Gottingen, Institute fur Anorganische Chemieder Universitat, Gottingen, Germany, 1999-2003.

[63] G. M. Sheldrick, *Acta Cryst*., 2008, **A64,** 112.

[64] R. Ahlrichs, M. Bär, M. Häser, H. Horn and C. Kölmel, *Chem. Phys. Lett.,* 1989, **162**, 165.

[65] A. Bauzá, A. Terrón, M. Barceló-Oliver, A García-Raso and A. Frontera, *Inorg. Chim. Acta.,* 2015, DOI: 10.1016/j.ica.2015.04.028; b) D. Sadhukhan, M. Maiti, G. Pilet, A. Bauzá, A. Frontera, S. Mitra, Eur. *J. Inorg. Chem.,* 2015, **11**, 1958; c) M. Mirzaei, H. Eshtiagh-Hosseini, Z. Bolouri, Z. Rahmati, A. Esmaeilzadeh, A. Hassanpoor, A. Bauza, P. Ballester, M. Barceló-

Oliver, J. T Mague, Behrouz Notash and A. Frontera, *Cryst. Growth Des*., 2015, **15**, 1351; d) P. Chakraborty, S. Purkait, S. Mondal, A. Bauzá, A. Frontera, C. Massera and D. Das, *CrystEngComm.,* 2015, **17**, 4680.

[66] S. F. Boys and F. Bernardi, *Mol. Phys*., 1970, **19**, 553.

[67] J. Contreras-García, E. R. Johnson, S. Keinan, R. Chaudret, J-P.Piquemal, D. N. Beratan, W. Yang, *J. Chem. Theory and Comput.,* 2011 **7 (3)**, 625.

[68] S. K. Wolff, D. J. Grimwood, J. J. McKinnon, D. Jayatilaka, M. A. Spackman, Crystal Explorer 3.1, University of Western Australia, Perth, Australia, 2007, http://hirshfeldsurfacenet.blogspot.com.

[69] J. J. McKinnon, D. Jayatilaka, M. A. Spackman, *Chem. Commun.,* 2007, 3814.

[70] R. Biswas, P. Kar, Y. Song, A. Ghosh, *Dalton Trans.,* 2011, **40**, 5324.

[71] B. Dutta, P. Bag, U. Florke, K. Nag, *Inorg. Chem*., 2005, **44**, 147.

[72] S. Banthia, A. Samanta, *J. Phys. Chem. B*, 2006, **110,** 6437.

[73] W. Chen, Q. Peng, Y. Li, *Cryst. Growth Des.,* 2008, **8**, 564.

[74] Z. Li, A. Dellali, J. Malik, M. Motevalli, R.M. Nix, T. Olukoya, Y. Peng, H. Ye, W.P. Gillin, I. Herna´ndez, P.B. Wyatt, *Inorg. Chem*., 2013, **52**, 1379.

[75] S. Majumder, L. Mandal, S. Mohanta, *Inorg. Chem*., 2012, **51**, 8739.

[76] P. Yang, X.X. Wu, J.Z. Huo, B. Ding, Y. Wang, X.G. Wang, *CrystEngComm*., 2013, **15,** 8097.

[77] a) P. Politzer, J. S. Murray, T. Clark, *Phys. Chem. Chem. Phys*., 2010, **12**, 7748; b) L. M. Azofra, I. Alkorta, S. Scheiner, *Theor. Chem. Acc*., 2014, **133**, 1586; c) A. Bauza, R. Ramis, A. Frontera, *J. Phys. Chem. A*, 2014, **118**, 2827; c) A. Bauzá, T. J. Mooibroek, A. Frontera, *Chem.*

Commun., 2015, **51**, 1491; d) G. Sánchez-Sanz, C. Trujillo, M. Solimannejad, I. Alkorta, J. Elguero, *Phys. Chem. Chem. Phys.,* 2013, **15**, 14310; e) J. E. Del Bene, I. Alkorta, J. Elguero, *J. Phys. Chem. A*, 2013, **117**, 6893.

Table1 Crystal parameters and selected refinement details for complexes 1 and 2

Compound	**1**	**2**
Empirical formula	$C_{38}H_{40}Cd3N_6O_{14}$	$C_{21}H_{30}CdCl_2N_2NiO_7$
Formula weight	1141.99	664.47
Temperature (K)	296(2)	273
Crystal system	Monoclinic	Monoclinic
Space group	$P2_1/c$	P 21/n
a (Å)	20.0254(6)	10.2934
b (Å)	8.8925(2)	15.9246(5)
c (Å)	23.9742(6)	15.9021(5)
α(°)	90	90
β(°)	100.745(1)	102.203(2)
γ(°)	90	90
Volume (Å^3)	4194.37(19)	2547.75(15)
Z	4	4
D_{calc} (g cm^{-3})	1.809	1.685
Absorption coefficient (mm^{-1})	1.518	1.821
F(000)	2264	1304
θ Range for data collection (°)	1.03-24.55	1.83-30.23
Reflections	58462	43947

collected		
Independent reflections / R_{int}	6990/0.0324	7304/0.0310
Observed reflections [I>2σ(I)]	5933	5773
Data / restraints / parameters	6990/ 0/553	7304/1/319
Goodness-of-fit on F^2	1.027	1.043
Final indices[I>2σ(I)]	R1 = 0.0238; wR2 = 0.0622	R1 = 0.0351; wR2 = 0.0936.
R indices (all data)	R1 = 0.0320; wR2 = 0.0736	R1 = 0.0485; wR2 = 0.1025
Largest diff. peak / hole (e $Å^{-3}$)	0.450/-0.312	1.217/-0.513

Table2. Selected bond lengths (Å) and bond angles (°) for complex **1**

Complex 1

Cd3–O1	2.744(3)	Cd3–O1A	2.762(3)
Cd3 –O2	2.260(2)	Cd3 –O2A	2.276(2)
Cd3 –O3	2.243(3)	Cd3 –O3A	2.268(2)
Cd3 –O4	2.495(3)	Cd3 –O4A	2.521(2)
Cd1–N1	2.241(3)	Cd2–N1A	2.237(3)
Cd1 –N2	2.257(3)	Cd2 –N2A	2.262(3)
Cd1 –O2	2.235(2)	Cd2 –O2A	2.216(2)
Cd1 –O3	2.224(2)	Cd2 –O3A	2.215(2)

Cd1 –O5	2.543(4)	Cd2 –O5A	2.474(3)
Cd3----Cd1	3.556	Cd3----Cd2	3.546
O1– Cd3–O2	61.41(7)	O1A– Cd3–O2A	60.34(8)
O2– Cd3–O3	73.85(8)	O2A– Cd3–O3A	73.70(8)
O3– Cd3–O4	66.23(8)	O3A– Cd3- O4A	65.41(8)
N1– Cd1–N2	90.2(1)	N1A– Cd2–N2A	88.4(1)
N1– Cd1–O2	83.49(9)	N1A– Cd2–O2A	84.6(1)
N2–Cd1–O3	83.0(1)	N2A–Cd2–O3A	82.28(9)
O2–Cd1–O3	74.70(8)	O2A–Cd2–O3A	75.91(8)
O5–Cd1–O6	51.7(1)	O5A–Cd2–O6A	50.9(1)
Cd3–O2–Cd1	104.54(8)	Cd3–O2A–Cd2	104.27(9)
C9-C10-C11	116.10	Cd3–O3A–Cd2	104.59(8)
C9A-C10A-C11A	121.15		

577 Table 3. Selected bond lengths (Å) and bond angles (°) for complex **2**

Complex 2

Ni1–N1	2.026(3)	Ni1–O1	2.003(2)
Ni1 –N2	2.033(3)	Ni2 –O3	1.993(2)
Cd1–O1	2.262(2)	Cd1–O2	2.528(2)
Cd1 –O3	2.257(2)	Cd1–O4	2.525(3)
Ni1–O5	2.158(3)	Cd1–Cl1	2.4811(8)
Ni1 –O6	2.142(3)	Cd1–Cl2	2.452(1)
Ni1----Cd1	3.390		

N1–Ni1–N2	98.7(1)	N1– Ni1–O1	90.5(1)
O3– Ni2–N2	91.1(1)	Cl1– Cd1–O2	86.59(6)
N1– Ni1–O3	169.5(1)	O1– Ni1–O3	79.94(9)
O1– Cd1–O3	69.25(8)	O3– Cd1–O4	65.45(8)
O1– Cd1–O2	65.39(8)	Cl1– Cd1–Cl2	120.42(3)
C9-C10-C11	115.8(5)	Cl1– Cd1–O4	88.46(7)

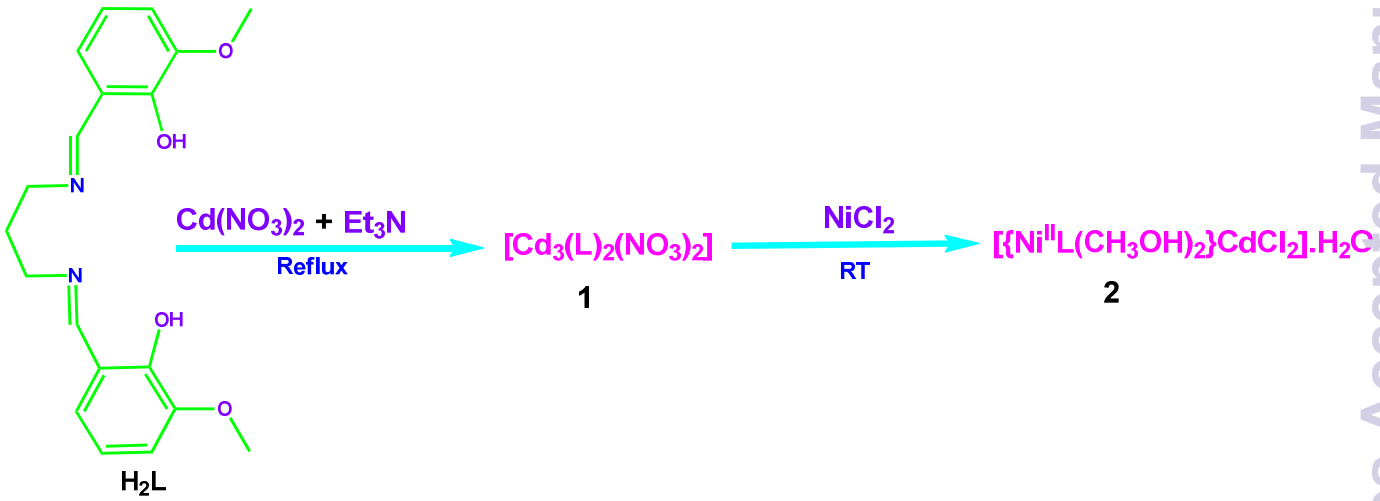

Scheme 1.The route to the syntheses of complexes **1** and **2**

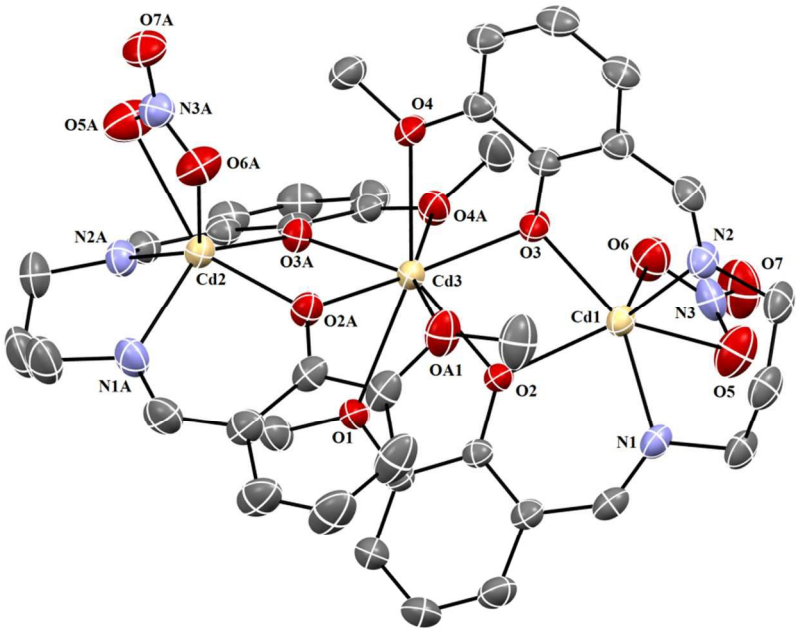

Fig. 1. Ortep view of compound **1**. Atoms are shown as 30% thermal ellipsoids. H atoms are omitted for clarity.

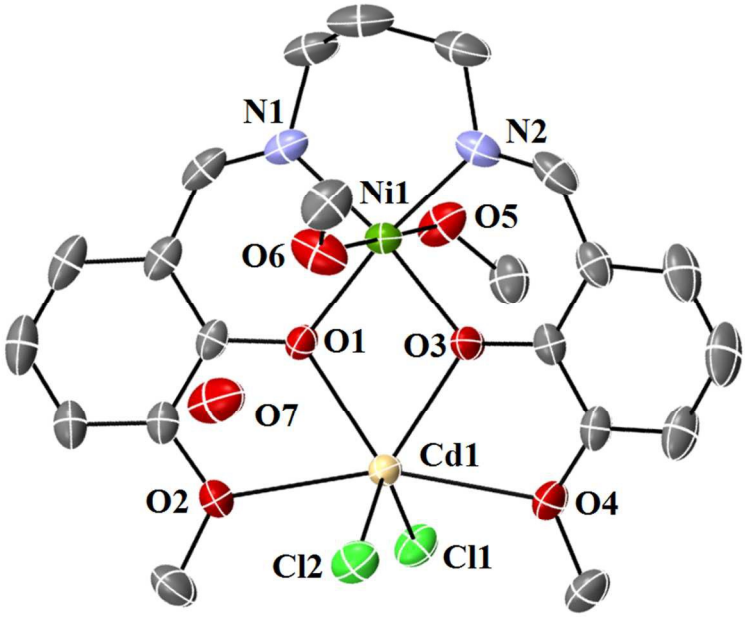

Fig. 2. Ortep view of compound **2**. Atoms are shown as 30% thermal ellipsoids. H atoms are omitted for clarity.

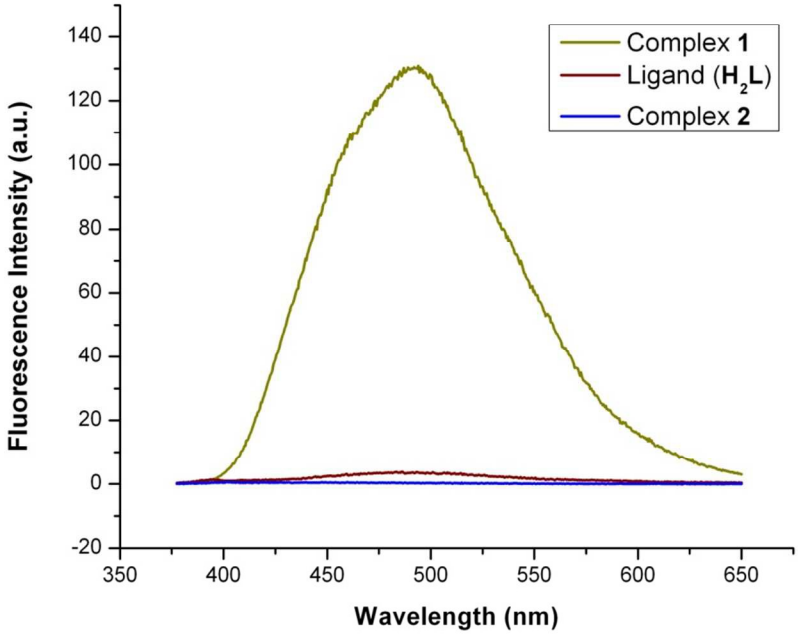

Fig. 3. Fluorescence emission properties of the Schiff base ligand **H_2L** and complexes **1** and **2** in DMF-CH_3CN (1:9, v/v).

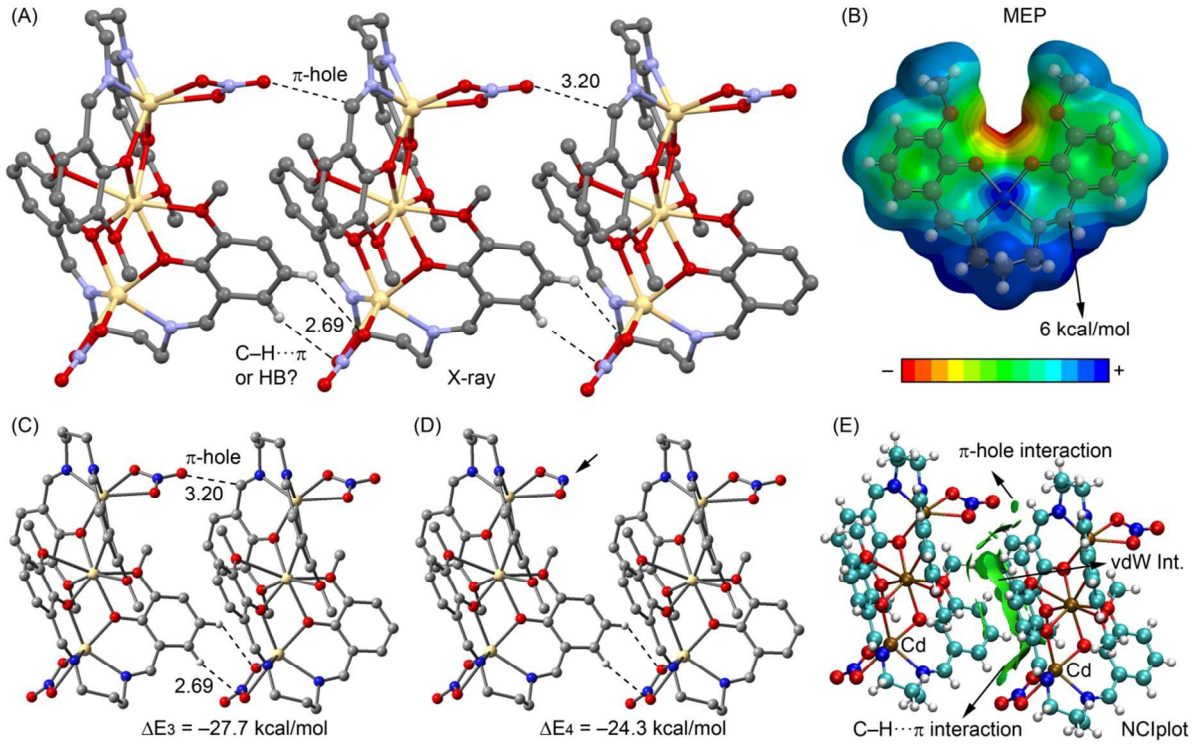

655

656

657 Fig. 4. (A) X-ray fragment of **1**. (B-D) Theoretical models used to evaluate the C–H···π, and H-
658 bonding interactions. Distances in Å. (E) MEP surface of a model compound of complex **1**. (F)
659 NCI plot of the dimer of compound **1**.

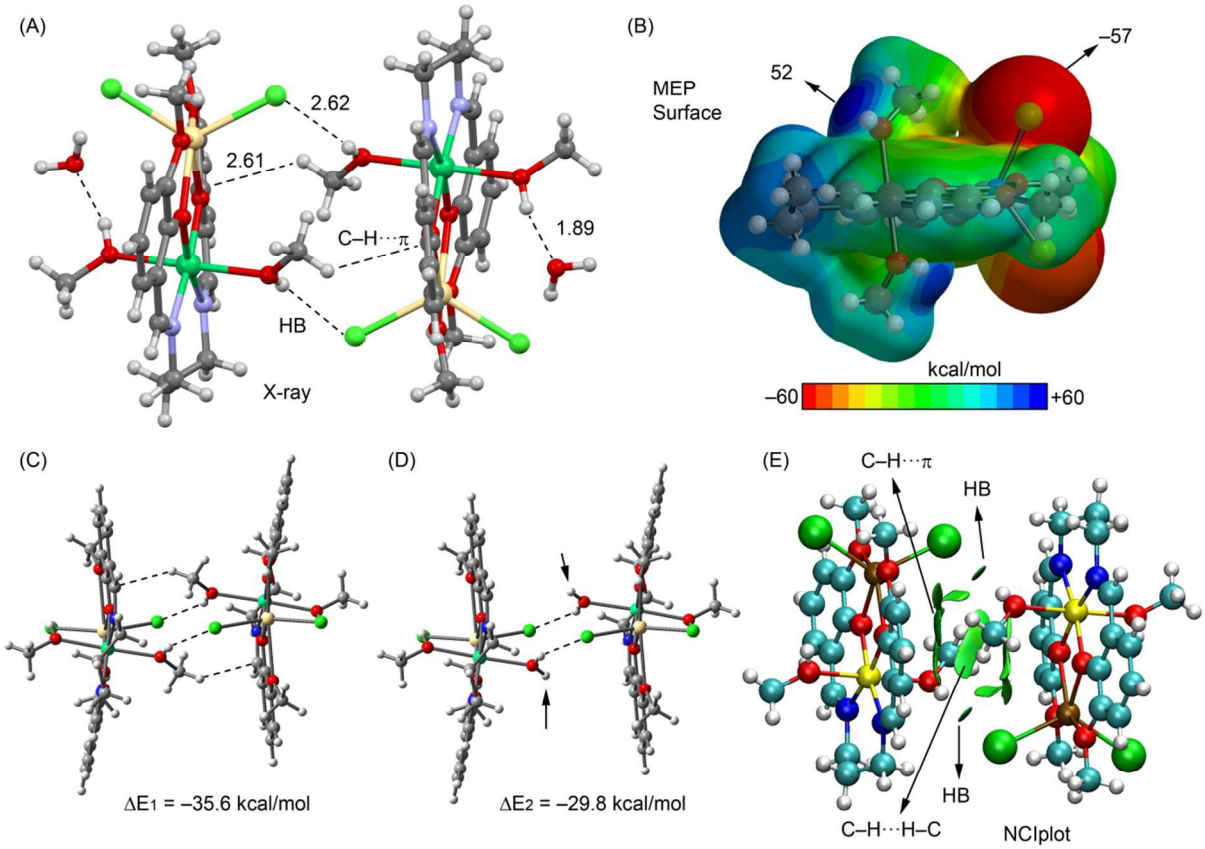

Fig. 5. (A) X-ray fragment of **2**. (B) MEP surface of compound **1**. (C,D) Theoretical models used to evaluate the non covalent interactions. Distances in Å. (E) NCI plot of the dimer of compound **2**.

Complex **1**	Complex **2**
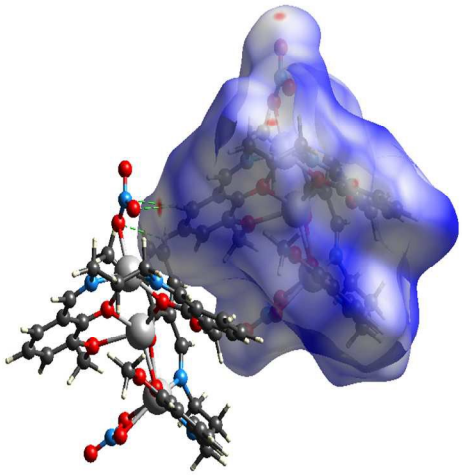	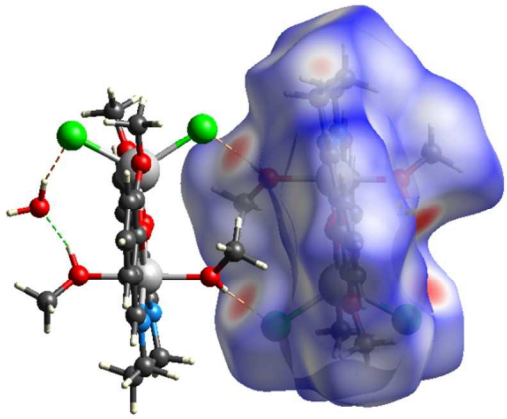

675

676 Fig. 6. Hirshfeld Surface mapped over d_{norm} for complexes **1** and **2.**

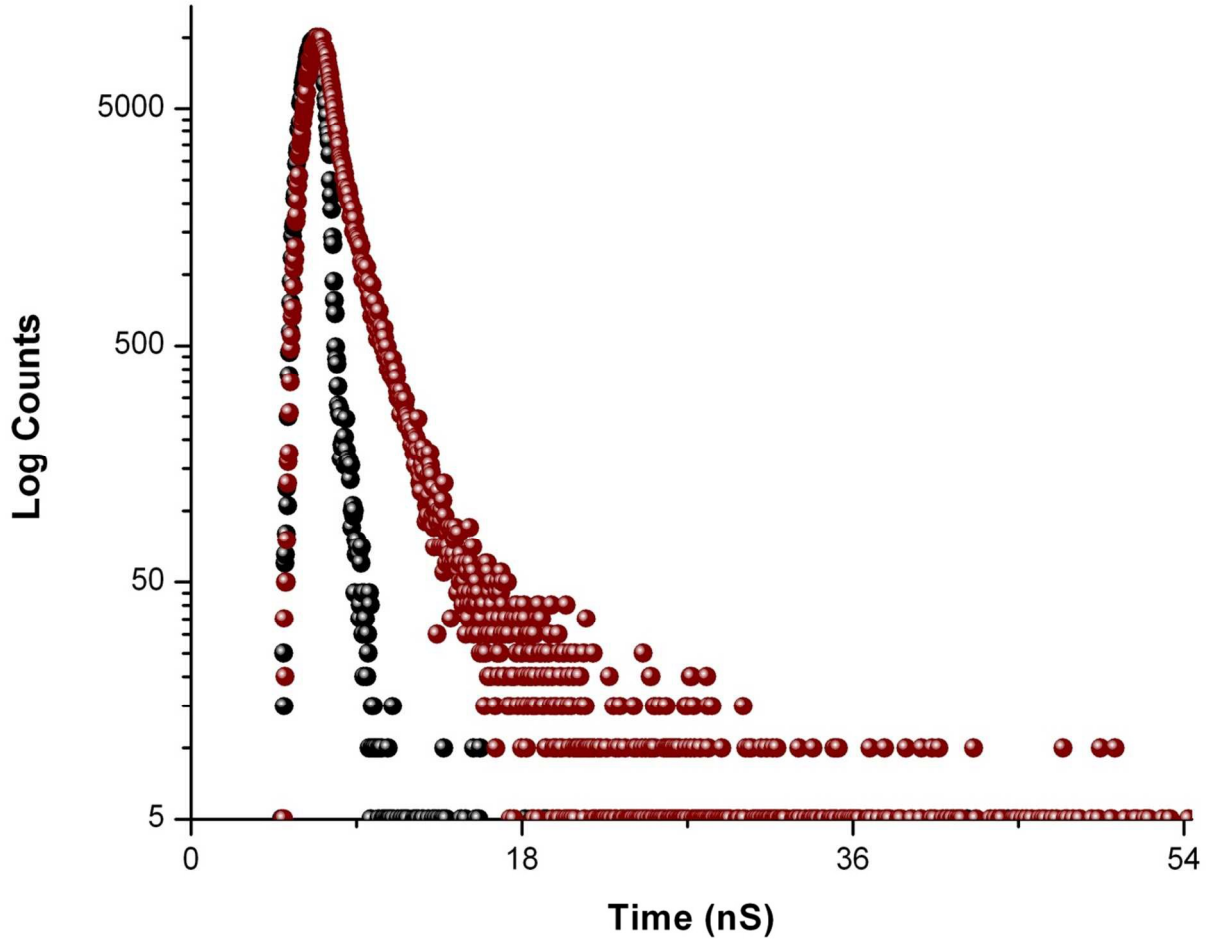

677

678 Fig. 7.Time-resolved fluorescence decay curves (logarithm of normalized intensity vs time in ns)
679 of Complex **1** (●) and (●) indicates decay curve for the scattered.

680

681

682

683

684

685

686

687

Graphical Abstract (Synopsis)

Exploration of unconventional π–hole and C–H···H–C types of supramolecular interactions in a trinuclear Cd(II) and a heteronuclear Cd(II)-Ni(II) complex and experimental evidence for preferential site selection of the ligand by 3d and 4d metal ions.

Saikat Banerjee,[a] Antonio Bauzá,[b] Antonio Frontera,*[b] and Amrita Saha*[a]

Abstract

In this present work we report synthesis and structural characterisations of a trinuclear cadmium (II) (**1**) and a di(phenoxido)-bridged dinuclear cadmium(II)–nickel(II) (**2**) complexes derived from a bicompertmental (N2O4) Schiff base ligand, **H_2L**. It has been observed that, in bicompertmental ligands the relatively small inner core is suitable for 3d metal ions and outer core can be occupied by different metal centers like 3d, 1s, 2s, 4d and 4f. We have experimentally established the above fact. In homotrinuclear complex **1** both inner (N2O2) and outer (O4) core has been occupied by cadmium (II) ions. Complex **1** upon reaction with $NiCl_2.6H_2O$ produces heterodinuclar complex **2**, where 3d nickel(II) ion easily replaced relatively large cadmium(II) ion. Structural studies reveal that, in complex **1** terminal Cd units acquire trigonal prismatic geometry whereas the central Cd unit is eight coordinated. In case of complex **2** both nickel(II) and cadmium(II) ions are hexa-coordinated in a distorted octahedral environment. Both the complexes are studied using different spectroscopic techniques. Complexes **1** and **2** exhibit important and relatively unexplored group of supramolecular interactions like π–hole, C–H···π and C–H···H–C along with other hydrogen bonding

interactions. Theoretical DFT calculations are devoted to analyze these noncovalent interactions. Several computational tools like MEP surface analysis and NCI analysis are utilized to explain and illustrate such interactions.

Graphical Abstract (Pictogram)

Saikat Banerjee,[a] Antonio Bauzá,[b] Antonio Frontera,*[b] and Amrita Saha*[a]